ELSEVIER

Polymer 43 (2002) 4217–4223

polymer

www.elsevier.com/locate/polymer

Characterisation of biaxial orientation gradients in poly(ethylene terephthalate) films and bottles using polarised attenuated total reflection FTIR spectroscopy

Neil Everall[a,*], Duncan MacKerron[b], Derek Winter[c]

[a]*ICI PLC, The Wilton Centre, Wilton, Redcar TS10 4RF, UK*
[b]*DuPont Teijin Films UK, The Wilton Centre, Wilton, Redcar TS10 4RF, UK*
[c]*DuPont Polyester Technologies, The Wilton Centre, Wilton, Redcar TS10 4RF, UK*

Abstract

Polarised attenuated total reflection (ATR) infrared spectroscopy has been used to quantify biaxial orientation in commercially manufactured poly(ethylene terephthalate) (PET) films and stretch-blow moulded bottles. Using a single-bounce accessory with a high refractive index element, and applying appropriate data normalisation prior to measuring band intensities, measurement of the average square direction cosines that describe the orientation is simple. Using this technique it was shown that uniaxially drawn PET films were actually biaxially oriented, and there were significant gradients in orientation through the film thickness. Bulk measurements, or methods that *assume* uniaxial orientation, would give incorrect results from these materials. The bottles exhibited complex orientation patterns that depended on preform and mould design, and again there were strong orientation gradients through the bottle walls. Kratky's model (pseudo-affine) was used in an attempt to predict the biaxial orientation gradients as a function of preform and bottle dimensions. © 2002 Published by Elsevier Science Ltd.

Keywords: Polymer; Orientation; Biaxial

1. Introduction and background

Quantification of molecular orientation in polymers is important for two main reasons. First, it provides a means of testing proposed deformation mechanisms, by comparing the theoretical and observed orientation parameters as a function of draw ratio. Second, orientation has a strong influence on structure/property relationships such as modulus, yield strain and tensile strength, and assists correlation of processing conditions with end-use properties. Characterising orientation involves measuring the distribution of polymer chains in a macroscopic co-ordinate system such as that in Fig. 1, where the extended chain axis is given by y, and the macroscopic axes are X, Y and Z. For a uniaxial system, if Y is the unique draw axis then only the polar angle θ is non-random. For biaxial systems (which, as we will show below, can arise under uniaxial draw conditions), both θ and ϕ are non-random.

Polarised infrared (IR) spectroscopy is widely used to determine second order orientation parameters. The fundamental parameter obtained is the average square direction cosine, or ASDC, given by $\langle\cos^2(yJ)\rangle$, where yJ denotes the angle between the chain axis y and the sample axis J. The P_2 value is given by $1/2\langle 3\cos^2\theta - 1\rangle = 1/2\langle 3\cos^2(yY) - 1\rangle$. In order to characterise a biaxial system it is generally necessary to measure three spectra with IR radiation polarised parallel to X, Y and Z, respectively. For a uniaxial system $\langle\cos^2(yX)\rangle = \langle\cos^2(yZ)\rangle$, and we need only to measure two spectra, one polarised along Y and the other along either X or Z.

A number of IR sampling methods have been described which permit these measurements. For thin films one can record spectra in transmission using the so-called 'tilted-film' method [1], which allows independent control of the X, Y and Z components. These studies are possible if the sample is sufficiently thin to avoid IR band saturation. For fundamental studies in the laboratory one can often produce samples that satisfy this requirement. However, when studying commercially fabricated articles one cannot choose the sample thickness, and for strongly absorbing materials such as aromatic poly(esters), the sample thickness almost always precludes simple transmission measurements. Microtoming thin sections and performing polarised IR microscopy is, in principle, a generic solution [2]. However,

* Corresponding author. Tel.: +44-1642-437637; fax: +44-1642-432244.
E-mail address: neil_everall@ici.com (N. Everall).

0032-3861/02/$ - see front matter © 2002 Published by Elsevier Science Ltd.
PII: S0032-3861(02)00247-1

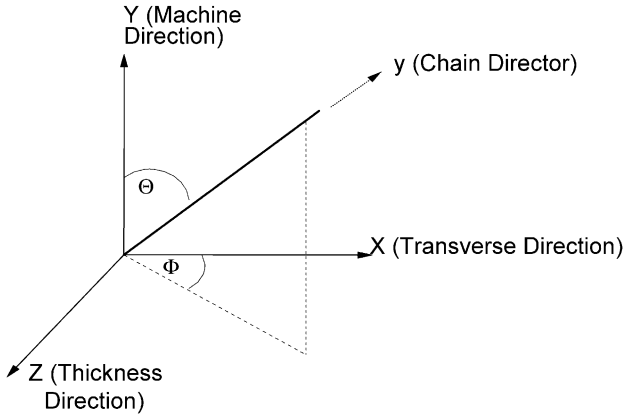

Fig. 1. Definition of macroscopic coordinate system.

it is time consuming, requires a high degree of operator skill (sections <5 μm thick are often required and are difficult to prepare), and the sectioning process can perturb the polymer morphology. However, once a cross section has been successfully prepared one can map or image property gradients through the wall of an article with excellent (~10 μm) spatial resolution.

IR reflection measurements offer alternative, non-destructive methods of measuring orientation, albeit restricted to the surface (~1–10 μm). Both specular reflectance and attenuated total reflection (ATR) measurements have been utilised [3–9]. Recently, Cole et al. [10] have shown that it is possible to characterise biaxially oriented poly(ethylene terephthalate) (PET) by using specular reflectance at near normal incidence. This is a significant advance, because previously it had been supposed that this geometry could not measure out-of-plane (OOP) orientation. However, specular reflectance measurements are restricted to materials that are sufficiently thick to prevent transflectance (i.e. radiation that penetrates the full thickness of the sample and is reflected from the rear sample–air interface back to the detector). When transflected light is present the observed spectrum is a distorted mixture of absorption and specular-reflection features, and is not useful for quantitative purposes. In some cases one finds that the polymer article is too thick for successful transmission spectroscopy, but too thin for specular reflectance (usually a thickness of many tens, and perhaps hundreds, of microns is needed to obtain good specular data). In contrast, the ATR method has general utility since it allows easy control of the *X*, *Y* and *Z* IR field components [6,7] and can be applied to articles ranging from a few μm up to several mm thickness. It involves holding the polymer surface in intimate contact with a high refractive index IR-transmitting prism, and controlling the polarisation of the IR beam. In the ATR configuration, only the surface of the polymer is sampled, so the absorption band intensities remain at a reasonable level irrespective of thickness.

Until recently, quantitative orientation analysis using ATR dichroism was difficult on two counts. First, in order to obtain self-consistent band intensities for all possible polarisation geometries, it was usually necessary to employ a special accessory that allowed a sample to remain clamped to the ATR element while it was rotated through 90 ° in the IR beam [11,12]. This was necessary to avoid disturbing the sample–prism contact area and perturbing the band intensities, but it has been suggested that this method can be unreliable [5,8,9]. The second problem is that the theory of Flournoy and Schaffers requires the polymer refractive indices, and these may not be known. Highly birefringent systems such as polyesters have refractive indices that strongly depend on orientation and crystallinity, so one cannot simply assume a typical reference value, the indices have to be independently determined for each sample. Fortunately, it has recently been shown that provided the IR spectrum contains a non-dichroic reference band, (i.e. one that is insensitive to orientation), then one can normalise the relevant band intensities to remove effects due to varying sample–prism contact [5]. Samples can then be unclamped and re-clamped without concern over changing the contact conditions. An additional benefit of normalisation is that it makes the analysis rather insensitive to the exact value of the polymer refractive index, such that a typical intermediate value can be safely assumed.

In previous work a single-bounce ATR unit (Golden Gate, Graseby-Specac, UK) was used to measure orientation in polymer films [5]. These results showed promise, but the method used a diamond ATR element with a fairly low refractive index (~2.4). This means that strong IR bands become distorted due to violation of the conditions for internal reflection (where the polymer refractive index exceeds that of the ATR element due to dispersion). It was suggested at the time that use of a higher-index element such as Germanium ($n \sim 4$) would reduce this dispersion and improve the accuracy of the results. The purpose of this current paper is threefold. First, a single bounce Ge-ATR unit is shown to significantly reduce band distortion compared with the diamond element. Second, this method is applied to stretched and blow-moulded PET articles (films, and bottles) to show how the orientation can vary significantly through the thickness of a wall, or at different points on a sample surface. Finally, we demonstrate that uniaxially drawn films can exhibit significant biaxial orientation.

2. Experimental

2.1. Samples

All samples used in these studies were fabricated from PET. Uniaxially drawn films were manufactured on a semi-technical scale film production unit (DuPont Teijin Films, Wilton, UK). The films were drawn at ~80 °C and then quenched on a cold-roll; the draw ratio (λ) ranged from 1.0 to 3.5 in 0.5 unit increments. The films were highly

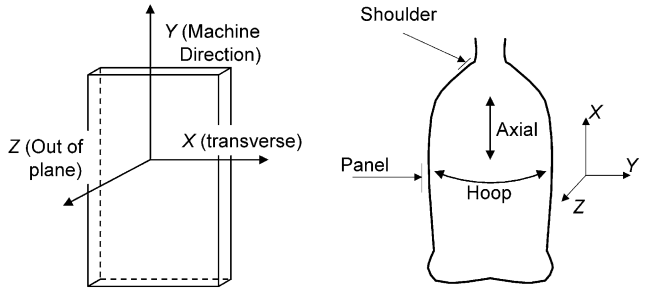

Fig. 2. Coordinate systems relevant to film and bottle geometry.

curved; spectra were recorded from both the inner and outer curved surfaces to check for orientation gradients. As examples of more complex articles, we analysed blow-moulded bottles of the type used to contain carbonated soft drinks. Four commercial sizes, namely 16 oz, 20 oz, 1 l and 2 l, were analysed.

The sample geometry is defined in Fig. 2. For the films we define the unique draw axis (machine direction) as *Y*, and the transverse direction as *X*. The OOP or thickness direction is denoted by *Z*. For the bottle, we assign *Y* to the Hoop, *X* to the Axial, and *Z* to the OOP directions, respectively. The 20 oz bottle was sampled in both the panel and the shoulder regions, while the other bottles were only analysed in the panel. Data were recorded from both the inner and outer surfaces of each of the bottle walls to check for property gradients.

2.2. Data acquisition

A single-bounce unit based on a Ge element ('SilverGate' Graseby-Specac, UK) was used for the ATR measurements, with a ZnSe polariser fitted to control the polarisation of the incident IR beam. The sampling area of the Ge element was about 1 mm^2, giving moderate spatial resolution for mapping purposes. Samples were clamped to the Ge element using a fixed-torque anvil, and spectra were recorded using a BioRad 375C FTIR spectrometer, with 200 scans at 4 cm^{-1} spectral resolution.

Fig. 3 shows the four arrangements that are required for

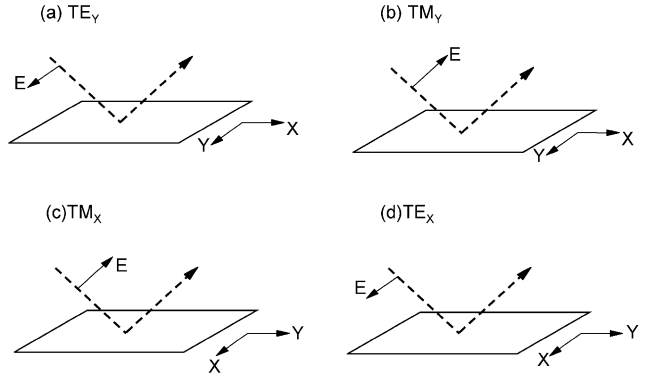

Fig. 3. The four possible sampling geometries for polarised ATR spectroscopy. See text for details.

the analysis. The incoming IR beam can be polarised either parallel to the plane of incidence (TM) or perpendicular to this plane (TE). The sample can be aligned with either the *X* or *Y* principal axes aligned perpendicular to the plane of incidence. These options can be written as TM_X TM_Y, TE_X and TE_Y, where the subscript denotes which of the sample axes lies perpendicular to the plane of incidence. A complete analysis involves recording spectra after each of the following steps: (a) Set the polariser to select TE radiation, clamp the sample such that the *Y* axis is perpendicular to the plane of incidence (TE_Y), (b) rotate the polariser through 90° (TM_Y), (c) unclamp the sample, rotate it through 90° (TM_X) and (d) rotate the polariser through 90° (TE_X).

3. Theory

The analysis required to extract the $\langle\cos^2(yJ)\rangle$ from ATR measurements is reported elsewhere [5]. The analysis of a biaxial material requires measurements of two IR bands, one with strong parallel dichroism (i.e. strong absorbance when the IR beam is polarised parallel to the extended chain), and one with perpendicular dichroism. The transition dipole angle β must be known, as it is for the PET bands used in this work (1017 cm^{-1}, $\beta \sim 20°$ ('parallel') 875 cm^{-1}, $\beta \sim 85°$ ('perpendicular'). The 1410 cm^{-1} band is non-dichroic and independent of crystallinity [13]. The band intensities were normalised relative to the 1410 cm^{-1} band to remove the effect of differing contact conditions when moving from the (TM_Y) to the (TM_X) configurations. The normalised 1017 and 875 cm^{-1} band intensities are converted into the orientation parameters using previously published equations, but note that there are minor errors in two of these equations as they were originally reported in Ref. [5]: the first bracketed term in the equation for P_{222} (Eq. (4)) should read $(1 + \cos^2\theta)$ rather than $(1 - \cos^2\theta)$, and in Eq. (13), the numerator should read $-4n_yn_z(1 - n_z^2/n_1^2 \sin^2\theta)$ rather than $-4n_yn_z(1 - n_x^2/n_1^2 \sin^2\theta)$.

4. Results and discussion

4.1. Comparison of Ge and diamond elements

Fig. 4 compares the spectra obtained for the 3.5 draw uniaxial film, obtained under TE_Y geometry, using single-bounce diamond and Ge elements. The diamond element yielded significant distortion of the strong bands, manifested as a 'derivative' shape with a poorly defined baseline. With the Ge element, the polymer refractive index never rises sufficiently to breach the conditions for total internal reflection, so the band was virtually undistorted. Therefore, we can be much more confident in using the Ge-ATR spectra for quantitative purposes. The data were extremely reproducible. For duplicate measurements on homogeneous materials, the $\langle\cos^2(yJ)\rangle$ agreed to within 0.01 units, and

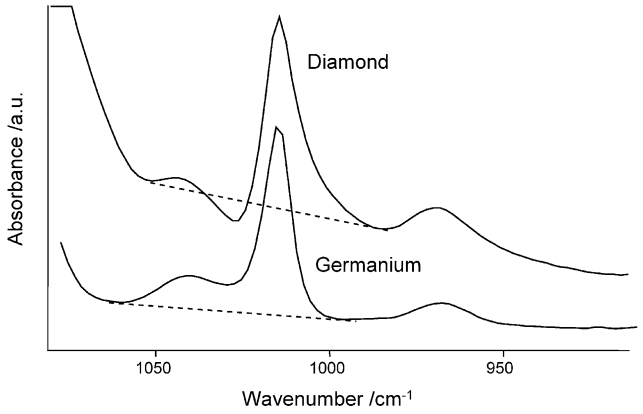

Fig. 4. Comparison of polarised ATR spectra of PET films, obtained with diamond and germanium reflection elements. Note the lower distortion with the germanium crystal.

five replicate measurements gave a precision of +/−0.002 (95% confidence).

4.2. Uniaxial film results

Turning now to property trends, Fig. 5 shows the P_2 values for each side of the uniaxially drawn films as a function of draw ratio. As expected the orientation increased with draw ratio, but there was also an orientation gradient through the thickness of the film, with the inner curved surface being more oriented. This gradient is not surprising since the film experiences significant temperature gradients during its manufacture (for example, contact with heated and cooled rolls). Fig. 6 shows an attempt to fit the data for the inner surface using two simple deformation models. Model (a) assumes affine deformation of a rubber network [14]. Model (b) is that due to Kratky [15] (later termed 'pseudo-affine' by Ward), which treats the chains as rigid rods which re-orient as the sample is deformed at constant volume. It yields the maximum theoretical orientation that can be obtained in the absence of segmental rotation and viscous relaxation, and as such it is expected to be more appropriate for predicting crystallite orientation in cold-drawn systems. Zbinden [16] has summarised the details

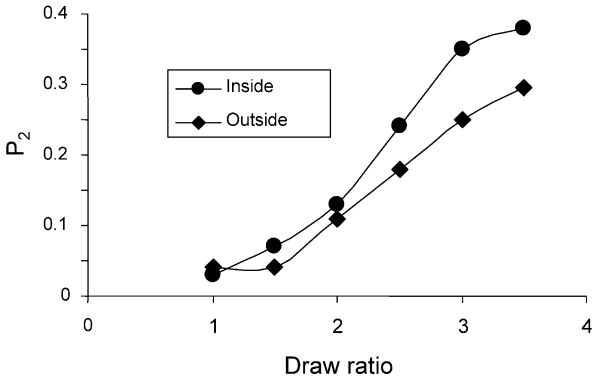

Fig. 5. Comparison of variation of P_2 versus draw ratio for inner and outer surfaces of uniaxially drawn films.

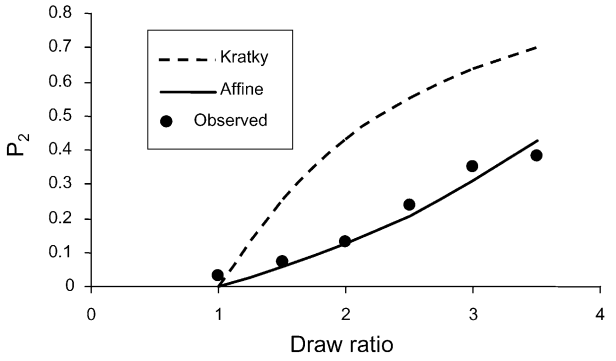

Fig. 6. Comparison of Kratky and affine deformation models for the uniaxial draw data. The affine model is clearly more appropriate.

of Kratky's model in convenient form, and the interested reader is referred to this text for more details. Using Kratky's model, assuming Y and X extensions of λ_Y and λ_X, the angular distribution function for a rigid chain is given by Eq. (1).

$$a(\theta,\phi)=\frac{\lambda_Y^3\lambda_X^3}{\left[[1+(\lambda_Y^3-1)\sin^2\theta]\left[1+(\lambda_X^3-1)\left[1-\dfrac{\lambda_Y^3\sin^2\theta\cos^2\phi}{\cos^2\theta+\lambda_Y^3\sin^2\theta}\right]\right]\right]^{3/2}} \tag{1}$$

The Hoop and Axial ASDCs are computed using Eqs. (2) and (3), respectively

$$\langle\cos^2(yY)\rangle=\frac{\int_0^{2\pi}\int_0^{\pi/2}\cos^2\theta\, a(\theta,\phi)\sin\theta\,\mathrm{d}\theta\,\mathrm{d}\phi}{\int_0^{2\pi}\int_0^{\pi/2}a(\theta,\phi)\sin\theta\,\mathrm{d}\theta\,\mathrm{d}\phi} \tag{2}$$

$$\langle\cos^2(yX)\rangle=\frac{\int_0^{2\pi}\int_0^{\pi/2}\sin^2\theta\cos^2\phi\, a(\theta,\phi)\sin\theta\,\mathrm{d}\theta\,\mathrm{d}\phi}{\int_0^{2\pi}\int_0^{\pi/2}a(\theta,\phi)\sin\theta\,\mathrm{d}\theta\,\mathrm{d}\phi} \tag{3}$$

For uniaxial draw the distribution function $a(\theta)$ is obtained by setting $\lambda_X=1$ in Eq. (1). The affine model predicts a linear relationship between P_2 and the strain function

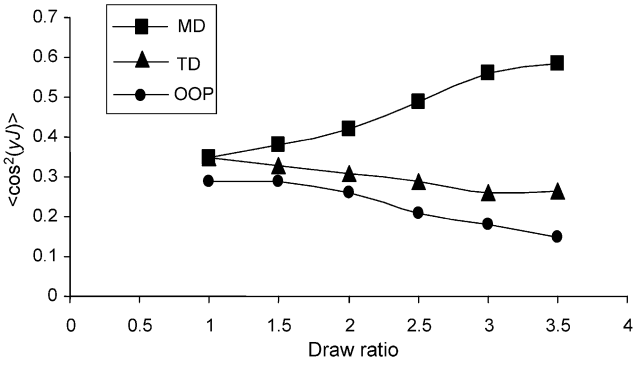

Fig. 7. Variation in MD, TD and OOP average square direction cosines for the uniaxially drawn films (inner surface) as a function of extension. Despite the nominal uniaxial draw, the film surface is biaxially oriented.

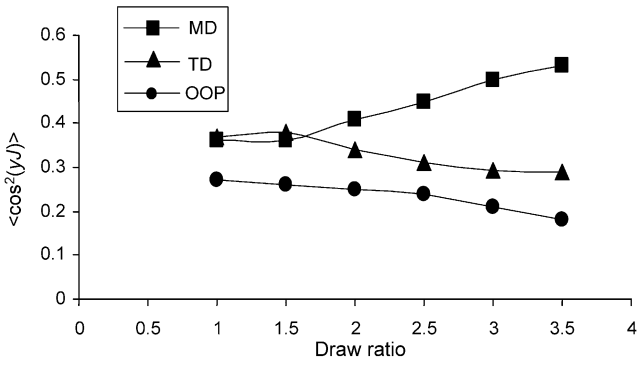

Fig. 8. Variation in MD, TD and OOP average square direction cosines for the uniaxially drawn films (outer surface) as a function of extension. Again, the film surface is clearly biaxially oriented.

$(\lambda^2 - 1/\lambda)$ for low extensions, with a gradient of $1/5N$, where N is the number of random links between network junction points [14].

Fig. 6 shows that the P_2 values for the PET films were modelled well by the affine model, assuming $N \sim 6$. In contrast, Kratky's model grossly over-estimated P_2. Cunningham et al. [17] also observed affine behaviour and inferred five random links between junctions. However, it is probably unwise to compare our value of N with the results of other workers, since the calculations assume a uniaxial system. In fact, this was not a valid assumption for these films. Figs. 7 and 8 compare $\langle\cos^2(yX)\rangle$, $\langle\cos^2(yY)\rangle$ and $\langle\cos^2(yZ)\rangle$ as a function of draw ratio for the inner and outer surfaces of the films. It is clear that the films were actually biaxially oriented at both surfaces, since the OOP orientation was significantly lower than the in-plane (TD) component. This shows how a system that has been uniaxially drawn can have biaxial structure; a subsequent analysis that *assumes* uniaxial orientation would be fundamentally flawed. One can rationalise why these films were biaxially oriented, since although they were drawn in the forward direction, the films passed over multiple rollers in the draw and post-draw regions and so lateral relaxation, particularly away from the edges of the material, was slightly constrained. Central regions of the film would therefore experience a strain field which approaches that in constant width drawing [18]. It is reasonable therefore that orientations in the X and Z directions could be different.

4.3. Bottle results

4.3.1. ATR measurements

When bottles are blown they undergo biaxial strain that varies over the bottle surface, so a complex orientation pattern is expected. Table 1 summarises the measured parameters for the 2 l, 1 l, 20 oz and 16 oz bottles. For the inner panel region of the 2 l bottle, the Hoop orientation was dominant, the OOP orientation was very small, and the Axial orientation was slightly less than random. At the outer surface, the Axial orientation increased but the Hoop orientation still dominated. Considering the in-plane 'balance' the Hoop/Axial orientation ratio (denoted 'Hoop/Axial') decreased from ~2.0 to 1.4 on moving from inner to outer wall. This behaviour is rationalised by considering the deformation that occurs on blowing a bottle. Bottles are blown from 'preforms', which are thick-walled tubes. Although the size and shape of a preform varies according to bottle design, in general, the inner wall suffers a larger Hoop extension than the outer wall during blow-moulding. In the panel region, typical Hoop extensions for a 2 l bottle are ~5 and 4 for the inner and outer surfaces, respectively. The Axial extension is typically ~2.5 for each surface in the same region. Therefore, it is not surprising that significant property gradients exist in bottle walls.

Table 1 also compares the $\langle\cos^2(yJ)\rangle$ for the 2 l bottle that were predicted using the Kratky model, assuming Hoop and Axial extensions of 5 and 2.5, respectively. On average, the model overestimated the Hoop orientation by ~17% and underestimated the Axial orientation by ~19%. In terms of orientation *changes*, it predicted an 11% fall and a 24% rise in Hoop and Axial orientations, respectively, on moving from the inner to outer surface, and a very low OOP orientation throughout. The observed changes were 15 and 23%, respectively, and the OOP orientation was much lower than the Hoop or Axial orientations throughout. Although in this case Kratky's model predicted the orientation parameters

Table 1
Orientation parameters for 2 l, 1 l, 16 oz and 20 oz bottles

Size	Position	$\langle\cos^2(yY)\rangle$ (Hoop)		$\langle\cos^2(yX)\rangle$ (Axial)		$\langle\cos^2(yZ)\rangle$ (OOP)	
		Observed	Predicted	Observed	Predicted	Observed	Predicted
2 l	Panel inside	0.63	0.72	0.31	0.25	0.06	0.03
2 l	Panel outside	0.54	0.64	0.38	0.31	0.08	0.05
16 oz	Panel inside	0.566	0.59	0.333	0.33	0.101	0.08
16 oz	Panel outside	0.429	0.53	0.441	0.37	0.131	0.10
1 l	Panel inside	0.539	–	0.389	–	0.072	–
1 l	Panel outside	0.307	–	0.580	–	0.113	–
20 oz	Panel inside	0.48	–	0.47	–	0.05	–
20 oz	Panel outside	0.39	–	0.57	–	0.04	–
20 oz	Shoulder inside	0.25	–	0.75	–	0	–
20 oz	Shoulder outside	0.27	X	0.73	X	0	X

and changes reasonably well, this will not always be the case, since the other factors will also influence the orientation, including blow rate/temperature, mould temperature/contact time, and polymer crystallinity. Knowledge of the extension ratios alone is not sufficient to reliably predict final orientations, hence the need to measure the $\langle\cos^2(\gamma J)\rangle$. However, Kratky's model was more effective when applied to the 2 l bottles than the uniaxial films. This could arise from the faster extension rates that the bottles experience, giving less time for relaxation, and also the fact that the bottles suffered larger draw ratios, and in this regime the affine and Kratky predictions become more similar.

The 16 oz bottle was blown using a preform and mould that yields, in the panel region, Hoop extensions of ~2.9 and 2.5 at the inner and outer walls, respectively, and an Axial extension of about 2.0 at both surfaces. Table 1 shows the expected pattern of decreasing Hoop and increasing Axial orientation on moving from the inner to the outer surface (Hoop/Axial ratio changed from ~1.7 to ~1.0). As expected from the lower extension ratios, the in-plane orientation was more balanced than with the 2 l bottle, particularly at the outer surface. The Kratky model predicted the orientation at the inner surface very well, but significantly overestimated the Hoop orientation at the outer surface. However, we stress that agreement between predicted and observed absolute values may be fortuitous since we have neglected the effect of viscous flow during blowing and relaxation.

Unfortunately we do not have the necessary information on preform design to estimate the extensions for the 1 l and 20 oz bottles, so we cannot predict the orientation parameters, but it is interesting to compare the observed values with those from the other bottles. First, the 1 l bottle had the now-familiar large orientation imbalance in favour of Hoop orientation at the inner surface (Hoop/Axial ~ 1.39), but at the outer surface the situation was completely reversed and the Axial orientation predominated (Hoop/Axial ~ 0.53). The dominant orientation direction rotated through 90° on moving through the bottle wall, a feature not observed for the 2 l or 16 oz articles. For the 20 oz bottle, the orientation pattern was different. At the panel inner surface, the in-plane orientation was well balanced, with Hoop/Axial ~ 1.0, but at the outer surface, Hoop/Axial ~ 0.7. Again, the OOP orientation was always very small. Orientation in the shoulder region bottle was very different to the panel, with very low Hoop orientation but strong orientation into the Axial direction. This result was surprising, since one would not predict significant extensions in this region. However, the result was reproducible and will be the subject of further investigation using bottles blown from a known preform design.

Although the ATR measurements are rapid and precise, they are restricted to the surface of the articles and so it is reasonable to ask how reliable they are and how indicative they might be of sub-surface properties. This can be investigated by microtoming thin sections from the wall (cut parallel to the Hoop or the Axial directions) and measuring property gradients using either point-mapping [2] or global imaging FTIR microscopy [19]. These approaches have been very useful in verifying and visualising orientation (and also crystallinity) gradients in bottles and films, and have validated the conclusions drawn from the ATR measurements. These studies will be reported in a future publication. An alternative approach, suggested by Cole et al. [10], is to remove successive thin layers of material by careful polishing, and to measure reflectance spectra from the exposed surface as it incrementally progresses through the material. Provided this does not perturb the polymer morphology it provides a method for depth profiling. Using this approach Cole et al. [10] studied a commercial PET bottle and they too observed significant orientation gradients through the wall thickness. In this case the Hoop orientation remained almost constant while the Axial orientation doubled on moving from the inside to the outside surface. Cakmak and Spruiell [20] used wide angle X-ray scattering and optical birefringence to study bulk and surface orientation in PET bottles. They too observed that the orientation varied significantly at different positions on the bottle surface, and also that the bottles were more highly oriented at the inner surfaces. Finally, we note that Mahendrasingam et al. [21] used a synchrotron to generate a microbeam of X-rays, and were able to map crystallinity and orientation gradients through the walls of PET containers, giving further evidence that morphology gradients are the norm in stretch blow moulded articles.

To summarise, the mechanical properties at any given point on a bottle will be largely determined by the molecular orientation, the polymer crystallinity and the wall thickness. The above results show that the molecular orientation varies significantly according to bottle design and the position on the surface, in agreement with previous work. This highlights the need to make spatially and surface-resolved orientation measurements in order to rationalise (and hopefully optimise) the bottle's end-use properties.

5. Conclusions

FTIR-ATR dichroism measurements, using a single-bounce Ge-ATR element, enable spatially resolved measurements of molecular orientation in complex articles fabricated from PET. The methodology should be applicable to any polymer system provided that the vibrational spectrum contains a non-dichroic band that can be used to normalise the spectra to remove the effect of variable contact area. This work has shown that even simple systems such as uniaxially drawn films can display significant orientation gradients and biaxial orientation. In such cases, transmission measurements made at normal incidence on the assumption of uniaxial alignment would yield incorrect conclusions.

The ATR technique was used to characterise orientation

patterns in blow moulded bottles, where strong biaxial orientation and large gradients occur over the surface and through the wall thickness. It can provide a valuable tool for relating microstructural, mechanical and end-use properties to the production conditions used to fabricate the bottles. Simple 'bulk average' measurements are wholly inappropriate for studying such systems, since they do not resolve the significant changes in orientation that can occur on moving through the bottle wall. Kratky's model for biaxial orientation was used as a simple (but rather approximate) tool for predicting changes in bottle orientation as a function preform design.

Acknowledgements

The authors thank ICI PLC, DuPont Teijin Films and DuPont Polyester Technologies for granting permission to publish this work.

References

[1] Koenig JL, Cornell SW, Witenhafer DE. J Polym Sci, Part A-2 1967;5:301.
[2] Chalmers JM, Croot L, Eaves JG, Everall N, Gaskin WF, Lumsdon J, Moore N. Spectrosc Int J 1990;8:13.
[3] Everall NJ, Chalmers JM, Local A, Allen S. Vib Spectrosc 1996;10:253.
[4] Cole KC, Guevremont J, Ajji A, Dumoulin MM. Appl Spectrosc 1994;48:1513.
[5] Everall N, Bibby A. Appl Spectrosc 1997;51:1083.
[6] Flournoy PA, Schaffers WJ. Spectrochim Acta 1966;22:5.
[7] Flournoy PA. Spectrochim Acta 1966;22:15.
[8] Mirabella FM. J Polym Sci, Polym Phys Ed 1984;22:1293.
[9] Mirabella FM. Appl Spectrosc 1988;42:1258.
[10] Cole KC, Daly HB, Sancchagrin B, Nguyen KT, Ajji A. Polymer 1999;40:3505.
[11] Hobbs JP, Sung CSP, Krishnan K, Hill S. Macromolecules 1983;16:193.
[12] Yuan P, Sung CSP. Macromolecules 1991;24:6095.
[13] Walls D. Appl Spectrosc 1991;45:1193.
[14] Ward IM. J Polym Sci, Polym Symp 1977;58:1.
[15] Kratky O. Kolloid Z 1933;64:213.
[16] Zbinden R. Infrared spectra of high polymers. New York: Academic Press, 1964. p. 189–225.
[17] Cunningham A, Ward IM, Willis HA, Zichy V. Polymer 1974;15:749.
[18] Gordon DH, Duckett RA, Ward IM. Polymer 1994;35:2554.
[19] Everall NJ, Chalmers JM, Kidder LH, Lewis EN, Schaeberle M, Levin I. Proc Am Chem Soc 2000;82:398.
[20] Cakmak M, Spruiell JE, White JL. Polym Engng Sci 1984;24:1390.
[21] Mahendrasingam A, Martin C, Bingham S, Fuller W, Blundell DJ. Adv X-ray Anal 2000;43:356.